

Dynamic conductivity of a lateral-surface superlattice in a magnetic field

This article has been downloaded from IOPscience. Please scroll down to see the full text article.

1995 J. Phys.: Condens. Matter 7 1101

(<http://iopscience.iop.org/0953-8984/7/6/011>)

View [the table of contents for this issue](#), or go to the [journal homepage](#) for more

Download details:

IP Address: 171.66.16.179

The article was downloaded on 13/05/2010 at 11:53

Please note that [terms and conditions apply](#).

Dynamic conductivity of a lateral-surface superlattice in a magnetic field

L I Magarill, I A Panaev and S A Studenikin

Institute of Semiconductor Physics, 630090, Novosibirsk, Russia

Received 20 July 1994, in final form 12 October 1994

Abstract. Results are presented of a theoretical and experimental investigation of the dynamic conductivity in the microwave region of a two-dimensional lateral-surface superlattice. A theoretical analysis based on the solution of the Boltzmann kinetic equation for 2D electrons in a laterally modulating potential, an external magnetic field and a microwave field shows that the components of the dynamic conductivity tensor have an oscillatory character of various types. A preliminary experimental study of the dynamic conductivity in the microwave region is presented. Measurements of the reflection coefficient of the microwave radiation ($f = 38$ GHz) from a GaAs/AlGaAs lateral superlattice have been carried out. For the first time Weiss-type oscillations have been observed in a dynamic regime.

1. Introduction

There has recently been considerable attention focused on periodically structured two-dimensional systems, such as surface-lateral superlattices, arrays of quantum dots and quantum wires, and arrays of antidots, which have unique physical properties. While investigating static magnetoresistance of microstructured 2D systems various effects have been observed. A novel type of oscillation (the so-called Weiss oscillation) has been discovered and intensively studied both experimentally and theoretically [1–13]. Furthermore, in the DC regime, the oscillations caused by the Aharonov–Bohm effect [14, 15] or selective orbits of ballistic electrons [16, 17], large negative magnetoresistances [18, 19] (in small magnetic fields) and positive magnetoresistances [20] (in high magnetic fields) have been found.

In far-infrared and Raman spectra, collective excitations of the electron gas manifest themselves [21, 22]. Recent work [23–26] indicates that laterally modulated electron systems may exhibit new dynamical properties of fundamental interest. Our paper is devoted to the theoretical and experimental investigation of the dynamic magnetoconductivity of a weakly modulated 2D electron gas in the microwave region.

2. Theory

The response of a system to an external electromagnetic field of cyclic frequency $\omega = 2\pi f$ is described by the dynamic conductivity tensor $\sigma_{ij}(\omega)$. In this section, expressions for components of the tensor σ_{ij} are derived. For this purpose we have generalized the approach developed in [13] for the calculation of the static magnetoresistance of a structure with 1D modulation to the case of a 2D superlattice in an external alternating electric field.

The expression for the dynamic conductivity is found on the basis of a solution of the Boltzmann kinetic equation for 2D electrons subject to a laterally modulating potential, an external constant magnetic field \mathbf{B} and a microwave field.

Assuming an external electric field $\mathbf{E}(t) = \text{Re}(\mathbf{E}_\omega e^{-i\omega t})$, where \mathbf{E}_ω is the complex amplitude of the electromagnetic field, we start from the linearized kinetic equation:

$$\tilde{\mathcal{L}}f_1 \equiv (\mathcal{L} - i\omega)f_1 = -e\mathbf{E}_\omega \mathbf{u}v(r, E) \frac{\partial f_0}{\partial \zeta} \quad (1)$$

$$\mathcal{L}f_1 = v(r, E)\mathbf{u}\nabla_r f_1 + \left(\nabla_r v(r, E) \frac{\partial \mathbf{u}}{\partial \varphi} + \omega_c \right) \frac{\partial f_1}{\partial \varphi} + \frac{1}{\tau} \left(1 - \int_0^{2\pi} \frac{d\varphi}{2\pi} \right) f_1. \quad (2)$$

Here f_1 is the non-equilibrium correction to the distribution function, which is linear in \mathbf{E}_ω ; the term $v(r, E) = \sqrt{2(E + eV(r))/m}$, where $V(r)$ is the lateral potential, which is a periodic function with period a_x and a_y along the corresponding axes; $e > 0$ is the absolute value of the electron charge, $\mathbf{u} = (\cos\varphi, \sin\varphi)$ (where φ is the polar angle of the electron velocity (momentum)), $\omega_c = eB/mc$ is the cyclotron frequency, τ is the relaxation time (as in [13], τ is assumed to be constant), and $f_0 = \{1 + \exp[(E - \zeta)/T]\}^{-1}$ is the Fermi function (where ζ is the chemical potential). Equation (1) is written in variables $\mathbf{r} = (x, y)$, φ and E , where $E = mv^2/2 - eV(r)$ is the total electron energy.

The complex amplitude of the current is expressed in terms of f_1 as

$$\mathbf{j} = -eN \langle f_1 \mathbf{u}v(r, E) \rangle \quad (3)$$

where $N = m/\pi\hbar^2$ is the density of states of an unmodulated 2D electron gas. Angular brackets denote the following operation:

$$\langle \dots \rangle = \int dE \int_0^{2\pi} \frac{d\varphi}{2\pi} \int \frac{d\mathbf{r}}{\Omega} (\dots) \quad (4)$$

where Ω is the 'volume' of the lateral superlattice elementary cell.

We introduce the function $F(r, E)$ as follows:

$$f_1 = e \frac{\partial f_0}{\partial \zeta} \sum_{i,j} \left(\frac{2v(r, E)u_i}{v_0^2(E)} + F_i \right) \tilde{D}_{ij}(E) E_{\omega j} \quad (5)$$

where $\tilde{D}_{ij}(E) = \tilde{D}_0(E)\tilde{d}_{ij}(E)$ is the unperturbed (i.e. in the absence of a lateral potential) dynamic diffusion tensor of a 2D system for electrons with an energy equal to E , $\tilde{D}_0(E) = [\tau v_0^2(E)/2](1 + \tilde{\gamma}^2)^{-1}$, $\tilde{d}_{xx} = \tilde{d}_{yy} = 1$, $\tilde{d}_{yx} = -\tilde{d}_{xy} = \tilde{\gamma}$, $\tilde{\gamma} = \omega_c\tau/(1 - i\omega\tau)$, and $v_0(E) = \sqrt{2E/m}$. The first term in (5) gives the (Drude-type) dynamic conductivity of an unmodulated 2D electron gas:

$$\tilde{\sigma}_{ij}^{(0)} = Ne^2 \int dE \frac{\partial f_0}{\partial \zeta} \tilde{D}_{ij}(E). \quad (6)$$

The second term leads to the correction due to $V(r)$:

$$\Delta\tilde{\sigma}_{i,j} = Ne^2 \sum_k \left\langle \frac{\partial f_0}{\partial \zeta} u_i \tilde{F}_k \tilde{D}_{kj}(E) \right\rangle. \quad (7)$$

From (1) one can obtain the equation for the function F . It has the form

$$\tilde{\mathcal{L}}F = -\frac{e\nabla_r V}{E}. \tag{8}$$

In the derivation of (8) the identity $u_k u_l + \partial u_k / \partial \varphi \partial u_l / \partial \varphi = \delta_{kl}$ has been used. After simple but cumbersome transformations the expression (7) for $\Delta \tilde{\sigma}_{ij}$ can be presented in the form

$$\Delta \tilde{\sigma}_{ij} = Ne^2 \sum_{k,l} \left\langle \frac{\partial f_0}{\partial \zeta} u_i \tilde{D}_{ik}(E) \frac{\nabla_k V}{E} \tilde{F}_l \tilde{D}_{lj}(E) \right\rangle. \tag{9}$$

We shall use the lateral potential in the simple form†

$$V(\mathbf{r}) = \sqrt{2}[V_x \sin(q_x(x)) + V_y \sin(q_y(y))] \tag{10}$$

where $q_{x,y} = 2\pi/a_{x,y}$. We assume the potential amplitudes $V_{x,y}$ to be weak, which allows us to solve (8) perturbatively. To first order in $V_{x,y}$ the function F is determined by

$$\tilde{\mathcal{L}}_0 F = -e\nabla_r V/E$$

with $\tilde{\mathcal{L}}_0 = \tilde{\mathcal{L}}|_{V=0}$. This equation can be solved by means of a Fourier series expansion over \mathbf{r} . Inserting the solution to (9) we find the following for the diagonal component of $\tilde{\sigma}_{ij}$ (note that we consider the case of a square superlattice: $a_x = a_y \equiv a$, $V_x = V_y \equiv V_0$; furthermore, we assume the electron gas to be strongly degenerate, i.e. $T = 0$ and $\partial f_0 / \partial \zeta \rightarrow \delta(E - E_F)$, where $E_F = \zeta(T = 0)$ is the Fermi energy):

$$\tilde{\sigma}_{xx}(\omega, B) = Ne^2 \tilde{D}_0 [1 + (\tilde{\gamma}^2 - 1)\tilde{K}] \tag{11}$$

$$\tilde{K} = \frac{(ql\epsilon)^2}{2\eta(1 + \tilde{\gamma}^2)} \frac{\tilde{S}(qv_F/\omega_c)}{1 - \tilde{S}(qv_F/\omega_c)} \tag{12}$$

$$\tilde{S}(z) = \eta \sum_{k=-\infty}^{\infty} \frac{J_k^2(z)}{k^2 \gamma^2 + \eta^2}. \tag{13}$$

Here $J_k(z)$ are Bessel functions, $\gamma = \omega_c \tau$, $\tilde{\gamma} = \gamma/\eta$, $\eta = 1 - i\omega\tau$, $l = v_F \tau$ is the free path length, $v_F \equiv v_0(E_F)$ is the Fermi velocity, $\epsilon = eV_0/E_F$ is a dimensionless parameter that is characteristic of a modulating lateral potential, and $\tilde{D}_0 = \tilde{D}_0(E_F)$. At $\omega = 0$ the complex values \tilde{D}_0 , \tilde{K} and \tilde{S} are reduced to corresponding real ones introduced in [13]. Equation (13) can be transformed to a form that is more convenient for numerical calculations:

$$\tilde{S}(z) = \frac{1}{\gamma \sinh(\pi\eta/\gamma)} \int_0^\pi d\varphi J_0(2z \sin \varphi) \cosh[\eta(\pi - 2\varphi)/\gamma]. \tag{14}$$

For σ_{yx} one can write the analogous expression

$$\sigma_{yx}(\omega, B) = Ne^2 \tilde{\gamma} \tilde{D}_0 (1 - 2\tilde{K}). \tag{15}$$

It is easy to verify that, at $\omega = 0$ for ρ_{yy} (where $\hat{\rho} = \hat{\sigma}^{-1}(0, B)$ is the static magnetoresistance tensor), one can derive from (11) and (15) the expression presented in [13].

Equations (11) and (15) were obtained in the limit of weak modulation, i.e. formally at $\epsilon^2 \ll 1$. However, it is necessary to note that for the applicability of the found expressions, the condition $|\Delta\sigma/\sigma| \ll 1$ ($\Delta\sigma = \sigma - \sigma|_{\epsilon=0}$) should be fulfilled, which is equivalent to $|(\tilde{\gamma}^2 - 1)\tilde{K}|$, $|\tilde{K}| \ll 1$. An analysis and numerical calculations show that these conditions can appear to be more rigid than $\epsilon \ll 1$.

† In many theoretical works (see, for example, [6, 7, 9]) a sinusoidal modulation potential has been used for the description of magnetotransport of lateral superlattices.

3. Numerical calculations

Using (11)–(14) we have carried out numerical calculations of the magnetic field dependencies of the value $\text{Re}(\Delta\sigma_{xx}(\omega, B)) = \text{Re}(\sigma_{xx} - \sigma_{xx}^{(0)})$, which is the correction to the real part of the conductivity due to the modulating potential (where $\sigma_{xx}^{(0)}$ is the conductivity of an unmodulated 2D electron gas), at different frequencies of an external electromagnetic field. In figure 1 we show some results of such calculations at magnetic fields up to 0.2 T. The range of magnetic fields (0 ~ 0.2 T) was chosen in an optimal way to demonstrate the novel and peculiar features of the dynamic conductivity in surface-lateral superlattices. The following parameters were used:

$$n_s = 4 \times 10^{11} \text{ cm}^{-2} \quad \mu = 2.5 \times 10^5 \text{ cm}^2 \text{ V}^{-1} \text{ s}^{-1} \quad a = 280 \text{ nm}$$

$$V_0 = 0.5 \text{ mV} \quad \epsilon = 0.035.$$

From figure 1 it is seen that the value $\text{Re}(\Delta\tilde{\sigma}_{xx})$ oscillates with the magnetic field; moreover, the oscillations have essentially different characters in different frequency regions. The ratio of the amplitude of oscillations to the total conductivity increases quadratically with ϵ and at $V_0 = 0.5 \text{ mV}$ approaches about 0.5%, 10%, 5%, 0.2% for curves (a), (b), (c) and (d), respectively.

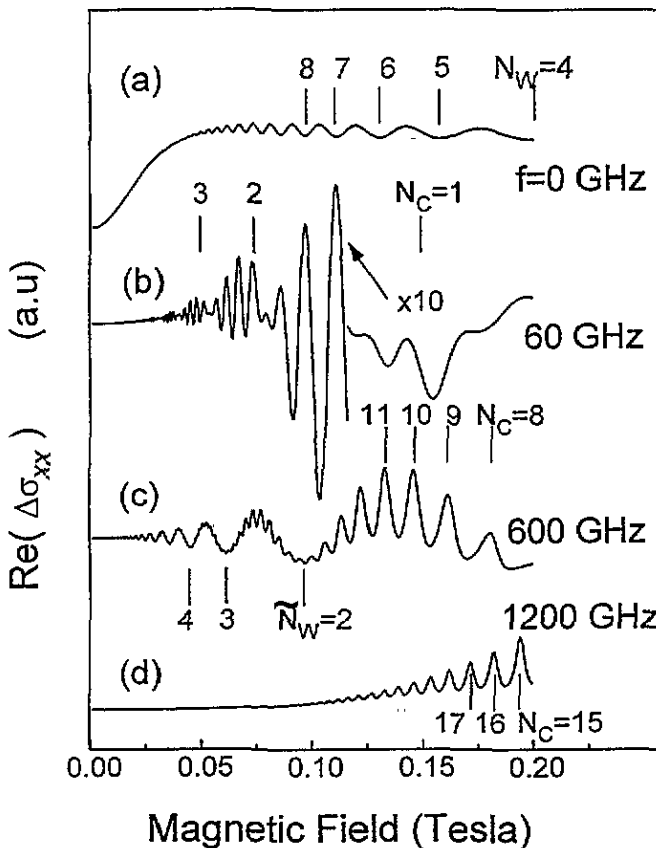


Figure 1. Correction to the real part of the dynamic conductivity of a lateral superlattice against magnetic field at different frequencies of an external electromagnetic field.

Curve (a) calculated at $f = 0$ points to the fact that modulating the potential of the lateral superlattice leads to oscillatory behavior of static magnetoconductivity (and naturally magnetoresistivity). These oscillations, referred to as Weiss oscillations [1–3], occur under commensurability with the cyclotron diameter $2R_c = 2v_F/\omega_c$ and superlattice period a . They have been studied experimentally and theoretically in a number of works [1–13]. Marks over curve (a) in figure 1 indicate the positions of minima of Weiss oscillations in magnetoconductivity. Corresponding values of the magnetic field are defined by the condition

$$2R_c/a = N_W - 1/4 \quad N_W = 1, 2, \dots \quad (16)$$

Under a higher frequency ($f = 60$ GHz; curve (b) in figure 1) there occur distinct beats: Weiss oscillations are modulated by an envelope function that is periodic in $1/B$. Extremal positions of the envelope function (loops), marked by ticks under the curve 2 in figure 1, correspond to the condition

$$\omega = N_C \omega_c \quad N_C = 1, 2, \dots \quad (17)$$

Therefore, the envelope function that modulates the amplitudes of Weiss oscillations is connected with a cyclotron resonance (CR) and its harmonics. CR harmonics are due to the lateral potential of the superlattice; under a classical description in an unstructured 2D system they are absent. Qualitatively, the appearance of CR harmonics can be explained by the fact that in the presence of a lateral potential the electron motion ceases to be harmonic with the only frequency ω_c . Note that in the region of CR harmonics with even orders of N_C , condition (16) corresponds to the positions of the minima of quick (i.e. Weiss) oscillations in $\text{Re}(\Delta\tilde{\sigma}_{xx})$, while for odd N_C , except in the vicinity of CR ($N_C = 1$), it defines maximal positions of this function. Thus, at transitions through nodes, phase jumps of Weiss oscillations close to π take place.

A further increase in frequency causes other oscillations to appear, periodic in $1/B$, which are associated with neither (17) nor (16). Curve (c) in figure 1, calculated at $f = 600$ GHz, shows such oscillations, which modulate more frequent oscillations: CR harmonics. Numerical calculations and theoretical analyses based on asymptotic properties of Bessel functions have demonstrated that the minima of the envelope function (curve (c) in figure 1) obey the following relation:

$$2R_c \Phi(f/f_{cr})/a = \tilde{N}_W - 1/4 \quad (18)$$

where $\tilde{N}_W = 1, 2, \dots$, $f_{cr} = v_F/a$, $\Phi(x) = \sqrt{1-x^2} - x \tan^{-1}(\sqrt{1/x^2-1})$. Equation (18) can be derived as follows. For $\xi = \omega\tau \gg 1$ and $\omega \geq 2\omega_c$ from (11) we can obtain that

$$\text{Re}(\Delta\tilde{\sigma}_{xx}(\omega, B)) \propto \sum_{k=-\infty}^{\infty} \frac{J_k^2(2\pi R_c/a)}{(k^2\gamma^2 - \xi^2 + 1)^2 + 4\xi^2} \quad (19)$$

At ω close to $n\omega_c$ the term $k = n$ gives the main contribution, i.e. $\text{Re}(\Delta\tilde{\sigma}_{xx}) \propto J_n^2(nf_{cr}/f)$. Using asymptotic expressions for Bessel functions [27] one can find that at $n \gg 1$ and $f < f_{cr}$

$$\text{Re}(\Delta\tilde{\sigma}_{xx}) \propto \frac{1}{nw} \cos^2[(w - \tan^{-1} w)n - \pi/4] \quad (20)$$

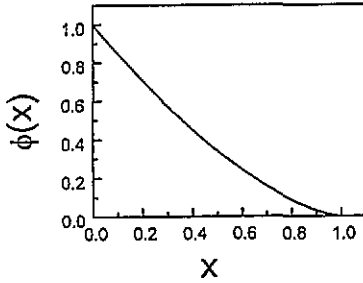


Figure 2. The frequency factor in (18).

where $w = \sqrt{(f_{cr}/f)^2 - 1}$. It is seen from (20) that $\text{Re}(\Delta\tilde{\sigma}_{xx})$ is a periodic function of n , with a period equal to $\pi/(w - \tan^{-1} w)$. Furthermore, it is not difficult to obtain (18).

The function $\Phi(x)$ is depicted in figure 2. The new oscillations gradually transform to static commensurability oscillations at zero frequency, when Φ is equal to 1, i.e. in this case condition (18) coincides with (16). Therefore the revealed oscillations can be referred to as *dynamic commensurability* or *dynamic Weiss* oscillations. Marks over curve (c) in figure 1 are set in accordance with (18).

These oscillations disappear when the frequency f of an external field is higher than f_{cr} (in the case of our chosen parameters $f_{cr} \approx 950$ GHz) and only CR harmonics are left with an exponential envelope function (see curve (d) in figure 1). This behaviour agrees with asymptotic expressions of Bessel functions at $n \gg 1$ and $f > f_{cr}$ [27]. In this case, instead of (20), one should really write

$$\text{Re}(\Delta\tilde{\sigma}_{xx}) \propto \left(1 - \frac{\tan^{-1} \bar{w}}{\bar{w}}\right) \frac{1}{n(\tanh^{-1} \bar{w} - \bar{w})} \exp[-2n(\tanh^{-1} \bar{w} - \bar{w})] \quad (21)$$

where $\bar{w} = \sqrt{1 - (f_{cr}/f)^2}$. The disappearance of oscillations at high enough frequencies can be understood crudely as follows. At $f > f_{cr}$, during the period of the external electromagnetic field $1/f$, the electron propagates a distance less than the superlattice period a , i.e. it doesn't 'feel' the periodicity of the modulating potential. Therefore, the commensurability oscillations disappear. CR harmonics remain because they are due to the perturbation potential (not necessarily periodical).

4. Experimental details

We attempted to study dynamic properties of a surface-lateral superlattice using microwave radiation.

The sample was fabricated from a selectively doped heterostructure GaAs/AlGaAs with a high-mobility two-dimensional electron gas having the following initial parameters at 4.2 K: $\mu = 2 \times 10^5 \text{ cm}^2 \text{ V}^{-1} \text{ s}^{-1}$ and $n_s = 4.0 \times 10^{11} \text{ cm}^{-2}$. On the surface of the heterostructure a mask, periodic along two directions, was covered by means of holographic photolithography with double exposition [18]. To create a potential relief, a wet etching of the structure to a depth of about 200 Å was performed. As a result, an initially homogeneous 2D electron gas was brought into the periodic superlattice potential with equal periods along both directions: $a = 280 \text{ nm}$ (the value a was tested with the help of a tunnelling microscope).

Measurements were carried out on the microwave setup shown schematically in figure 3. The microwave radiation (H_{10} wave, $f = 38$ GHz) from the source on the basis of a Gunn diode (1) propagated along a rectangular waveguide of cross section $3.4 \times 7.2 \text{ mm}^2$, passed

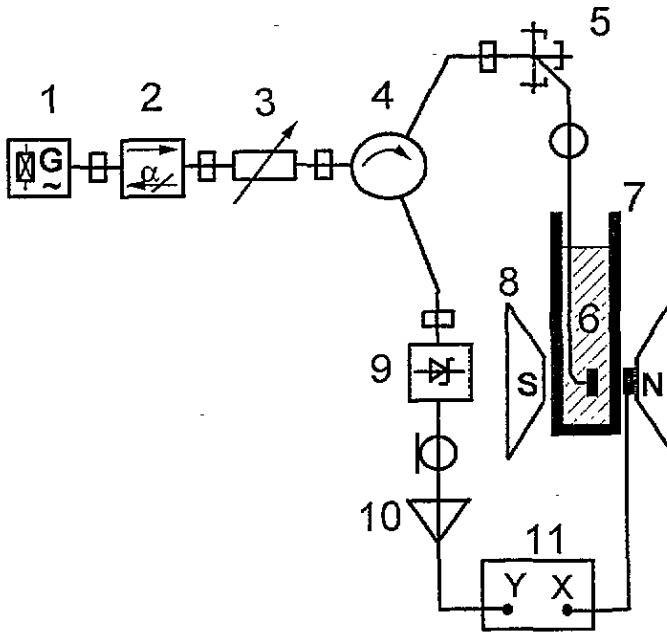


Figure 3. Experimental setup.

through isolator (2), attenuator (3) and microwave circulator (4), and then reached the T-shaped wave bridge (5), where the H_{10} wave was transformed into a H_{11} wave in a thin stainless-steel cylindrical waveguide of diameter 6 mm. The specimen (6) was mounted on the open end of the cylindrical waveguide in a helium cryostat (7) between poles of an electromagnet (8). The active layer of the sample was placed facing the waveguide, and behind the sample the metallic plate was attached. The reflected radiation propagated back along the waveguide, and was directed onto the microwave detector (9) by the circulator. After detection, the signal was amplified (10) and recorded by means of the two-coordinate XY recorder (11). To increase the sensitivity, we used the technique of weak modulation of the magnetic field with synchronous signal detection at the basic frequency [28]. Thus, the measured signal is proportional to the derivative of the reflectance with respect to the magnetic field dR/dB .

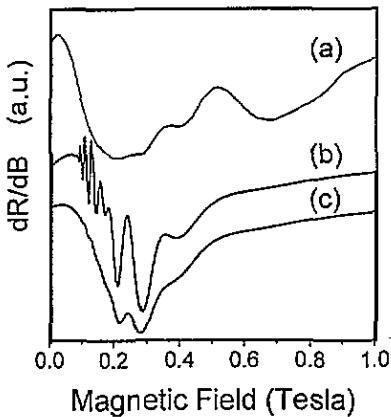


Figure 4. Magnetic field dependencies of the reflection coefficient from a GaAs/AlGaAs lateral superlattice. Curve (a): experiment; curves (b) and (c): theory.

Curve (a) in figure 4 shows the experimental magnetic field dependence of the derivative

of the reflection coefficient dR/dB for the surface superlattice structure described above. It is seen that oscillations occur on the background of the monotonic dependence of the reflection coefficient.

The observed oscillations cannot be explained by collective excitations: edge magnetoplasmons or 2D magnetoplasmons. Edge magnetoplasmons cannot be excited because the sample completely covers the waveguide cross section. For a sample with a perimeter about 1 cm they can manifest themselves at magnetic fields much lower than 1 kG [29]. As for 2D magnetoplasmons, their characteristic frequency at a wavevector $q = 2\pi/a \approx 2 \times 10^5 \text{ cm}^{-1}$ lies in the submillimeter region (a wavelength of about 150 μm) not in the microwave range [21]. Therefore, to explain the obtained experimental data, we used the single-particle approach based on the theoretical analysis described above.

Since in the experiment the reflectance was measured, we derived the expression for the microwave reflection coefficient taking into account the waveguide geometry. Maxwell's equations were solved in the simplest one-dimensional geometry (the direction of propagation of the wave is normal to the plane of a sample) with corresponding boundary conditions. It is assumed that a metallic plate placed behind the sample reflected the microwave radiation completely. In the case of a two-dimensional lateral superlattice with the same periods along both directions in the plane of the electron system, the reflection coefficient (assuming that the axis x is chosen along the polarization vector of an incidence wave) takes the form

$$R = \left| \frac{|A|^2 + 2(1 - A)\bar{\sigma}_{xx} - \bar{\sigma}_{xx}^2 - \bar{\sigma}_{yx}^2}{(A + \bar{\sigma}_{xx})^2 + \bar{\sigma}_{yx}^2} \right|^2 \quad (22)$$

where $\bar{\sigma}_{ij} = 4\pi\lambda_w\bar{\sigma}_{ij}/c\lambda$, $A = 1 + i \cot(kd)\lambda_w n/\lambda$, $k = 2\pi n/\lambda$ (where λ and λ_w are the wavelengths in the vacuum and the waveguide, respectively), and n and d are the refractive index and the substrate thickness. As may be seen from (22), in the general case the relation between R and $\bar{\sigma}_{ij}(\omega)$ is rather cumbersome. If the condition $|\bar{\sigma}_{ij}| \ll |A|$ is fulfilled, (22) can be simplified. We then get the following expression:

$$R = 1 - \frac{16\pi\lambda_w}{\lambda} \frac{\text{Re}(\bar{\sigma}_{xx}(\omega, B))}{|A|^2} \quad (23)$$

The required condition can be fulfilled at low carrier mobility or when $\cot(kd)$ is large enough, i.e. at a substrate thickness close to $l\lambda/2$ (where l is an integer). In our case the required conditions were not fulfilled. Therefore, for comparison of experiment with theory, we employed the expression (22).

The magnetic field dependence of the derivative of the reflection coefficient dR/dB obtained by numerical calculation using (11)–(13) with $\mu = 6 \times 10^4 \text{ cm}^2 \text{ V}^{-1} \text{ s}^{-1}$, $n_s = 3.8 \times 10^{11} \text{ cm}^{-2}$, $a = 280 \text{ nm}$, $V_0 = 2.0 \text{ mV}$ ($\epsilon = 0.15$) and $f = 38 \text{ GHz}$ is depicted in figure 4 (curve (b)). The parameters were chosen in an optimal way to correspond most closely to experimental data.

From figure 4 (curve (b)) it is seen that the theory predicts a large number of oscillations, while experimentally many fewer oscillations were observed (curve (a)). The inclusion of a finite temperature into the theory does not lead to the observed amplitudes of oscillation. For the closest agreement of experimental data with theory, one has to assume the existence of inhomogeneity over the surface of the structure, which results in a spread of cyclotron diameters and a sequence in smearing the oscillations. In our numerical calculations an

inhomogeneity was modelled as the inhomogeneity on carrier concentration, in the following manner:

$$\sigma_{ij} = \frac{1}{\pi} \int_{-\infty}^{\infty} \frac{\delta E_F}{[(E_F - E_{F0})^2 + \delta E_F^2]} \sigma_{ij}|_{E_F} dE_F \quad (24)$$

where $E_{F0} = n_{s0}/N$ and $\delta E_F = \delta n_s/N$. Curve (c) in figure 4 has been calculated using (11), (15) and (22), taking into account (24) at $\delta n_s/n_{s0} = 0.18$.

A satisfactory qualitative description of the oscillation amplitudes is achieved by assuming an inhomogeneity of about 20%. Such a large inhomogeneity is not surprising for a sample of about 1 cm^2 . However, we could not obtain good quantitative fitting. Apparently, this may be connected with the large potential amplitude in the sample under investigation, such that the developed theory becomes inapplicable.

5. Conclusion

In conclusion, we have carried out a theoretical analysis of the dynamic conductivity of a lateral superlattice by solving the classical kinetic equation. It was shown that the dependence of the dynamic conductivity on the external microwave field frequency exhibits different types of oscillations, periodic in a reciprocal magnetic field: CR harmonics, static and dynamic Weiss-type oscillations. The oscillations can superpose, resulting in a complicated picture of oscillations with beats. Experimental dependencies of the derivative of the reflectance from GaAs/AlGaAs surface-lateral superlattice are obtained. The dynamic commensurability oscillations in the microwave region at a frequency $f = 38 \text{ GHz}$ have been observed for the first time.

Acknowledgments

We thank P A Borodovskii for helpful discussions on microwave measurements. We also acknowledge A I Toropov and N T Moshegov for providing us with initial heterostructures. This work was partially supported by Russian Foundation for fundamental investigations (grants 93-02-15997 and 93-02-15715).

References

- [1] Weiss D, von Klitzing K, Ploog K and Weimann G 1989 *Europhys. Lett.* **8** 179
- [2] Gerhardt R R, Weiss D and von Klitzing K 1989 *Phys. Rev. Lett.* **62** 1173
- [3] Winkler R W, Kotthaus J P and Ploog K 1989 *Phys. Rev. Lett.* **62** 1177
- [4] Weiss D, von Klitzing K and Ploog K 1990 *Surf. Sci.* **229** 88
- [5] Gerhardt R R, Weiss D and Wulf U 1991 *Phys. Rev. B* **43** 5192
- [6] Zhang C and Gerhardt R R 1990 *Phys. Rev. B* **41** 12850
- [7] Peeters F M and Vasilopoulos P 1992 *Phys. Rev. B* **46** 4667
- [8] Weiss D, Roukes M L, Menschiig A, Grambow P, von Klitzing K and Weimann G 1991 *Phys. Rev. Lett.* **66** 2790
- [9] Oakeshott R B S and MacKinnon 1993 *J. Phys.: Condens. Matter* **5** 6991
- [10] Liu C T *et al* 1991 *Appl. Phys. Lett.* **58** 2945
- [11] Fang H and Stiles P 1990 *Phys. Rev. B* **41** 10171
- [12] Ensslin K and Petroff P M 1990 *Phys. Rev. B* **41** 12307
- [13] Beenakker C W J 1989 *Phys. Rev. Lett.* **62** 2020

- [14] Gusev G M et al 1992 *Sov. Phys.-JETP Lett.* **55** 123
- [15] Weiss D et al 1993 *Phys. Rev. Lett.* **70** 4118
- [16] Schuster R, Ensslin K, Kotthaus J P, Holland M and Standley C 1993 *Phys. Rev. B* **47** 6843
- [17] Baskin E M, Gusev G M, Kvon Z D, Pogosov A G and Entin M V 1992 *Sov. Phys.-JETP Lett.* **55** 678
- [18] Gusev G M, Kvon Z D, Besman V B, Vilms P P, Kovalenko N V, Moshegov N T and Toropov A I 1992 *Fiz. Tekh. Poluprov.* **26** 539
- [19] Berthold G, Smoliner J, Roskopf V, Gornik E, Böhm G and Weimann G 1992 *Phys. Rev. B* **45** 11350
- [20] Geim A K, Taboryski R, Kristensen A, Dubonos S V and Lindelof P E 1992 *Phys. Rev. B* **46** 4324
- [21] Heitmann D 1986 *Surf. Sci.* **170** 332
- [22] Goni A R, Pinczuk A, Weiner J S, Dennis B S, Pfeiffer L N and West K W 1993 *Phys. Rev. Lett.* **70** 1151
- [23] Lorke A 1992 *Surf. Sci.* **263** 307
- [24] Mikhailov S A 1993 *Pis. Zh. Eksp. Teor. Fiz.* **57** 570
- [25] Dahl C, Kotthaus J P, Nickel H and Schlapp W 1992 *Phys. Rev. B* **46** 15590
- [26] Dahl C, Kotthaus J P, Nickel H and Schlapp W 1993 *Phys. Rev. B* **48** 15480
- [27] Bateman H and Erdelyi A 1953 *Higher Transcendental Functions* vol 2 (New York: McGraw-Hill)
- [28] Studenikin S A and Skok E M 1986 *Phys. Status Solidi b* **134** 745
- [29] Volkov V A and Mikhailov S A 1991 *Landau Level Spectroscopy (Modern Problems in Condensed Matter Sciences 27.2)* ed G Landwehr and E I Rashba (Amsterdam: North-Holland) p 855